A multivariate analysis approach in determining potential hotspots of seasonal rainfall change over Uganda

Kevin John Oratungye[1,2], Christopher Oludhe[1], Moses Mwangi Manene[1], Everline Komutunga[2]

[1]University of Nairobi P.O. Box 30197 00100, Nairobi, Kenya
[2]National Agricultural Research Laboratories (NARL) P.O. Box 7065, Kampala, Uganda

Corresponding Author
Kevin John Oratungye, M.Sc.
Email: johnkevin067@gmail.com

Abstract

Evidence of climate change continues to emerge in Uganda as indicated by recent floods in Teso sub-region and Kasese district, landslides in Bududa and long droughts experienced in Karamoja. The major objective of the study was to identify potential hotspots of rainfall change in Uganda during March-May and October-December seasons. Monthly rainfall data for the period extending from 1951 to 2010 were used in the study. Geospatial Climate analysis (GeoCLIM) tool was used to determine geographical areas that have experienced changes in seasonal rainfall over the decades 1981-2010 relative to the long-term mean (1951-2010). Mbale, Mbarara and Moroto were identified as areas of potential rainfall change. The historical rainfall series for the identified areas were tested for inhomogeneities using Standard Normal Homogeneity and Pettitt tests and found to be homogenous. Multivariate two-sample Hotelling T^2-test was used to provide evidence of rainfall change in the identified areas by comparing mean seasonal rainfall vectors between the sub-periods 1951-1980 and 1981-2010. Results indicated a significant simultaneous decrease in mean rainfall over Moroto and Mbarara areas across the March-May season with April having the highest decrease (11 mm and 18 mm respectively). Mean rainfall in Mbale was found to have increased simultaneously across both wet seasons with April and October experiencing the greatest increase (10 mm apiece). Therefore hotspots of rainfall decrease were evident in Moroto (Karamoja) and Mbarara (Southwestern) whereas hotspots of rainfall increase were prominent in Mbale (Mt Elgon). There is need to account for disparity in rainfall patterns over Uganda by distinguishing between hotspots of unimodal and bimodal rainfall regimes.

Key words: Hotspots, rainfall, season, change, multivariate

Introduction

Evidence of climate change around the globe is emerging through increase in rainfall variability and the frequency of extreme weather events such as drought, floods and hurricanes, all which are very likely to be associated with the observed increase in anthropogenic greenhouse gas emissions (Intergovernmental Panel on Climate Change IPCC, 2007).

Climate change hotspots have been defined by Thornton *et al.,* (2008) as regions that are particularly at risk of suffering significant impacts from current or future climate change. This encompasses geographic areas projected to experience relatively large changes in temperatures and rainfall amounts and patterns. Hagenlocher *et al.,* (2014) defines hotspots as areas where extreme flood and drought events have occurred more frequently over the past three decades and trends in rainfall and temperature are evident, particularly during the wet seasons.

Uganda is one of the developing countries grappling with the impacts of climate change and variability as indicated by recent floods in Teso sub region and Kasese district, landslides in Bududa and long droughts experienced in the Karamoja; all of which have led to crop loss and subsequent famine and displacement of people (Government of Uganda GOU, 2010). As such, Uganda is vulnerable to climate change since majority of its population derive their livelihood from rain-fed agriculture (Mukiibi, 2001).

According to Phillips and McIntyre (2000), Uganda experiences two major rainfall regimes namely bimodal and unimodal. The bimodal regime is observed over majority of the country such as the southern region and areas near the equator with the first wet season occurring in March-May (MAM), also known as 'long-rains'. The second wet season takes place in October-December (OND) and is also known as 'short-rains'. The unimodal pattern on the other hand dominates areas far north of Uganda where the two wet seasons merge forming one long wet season from April-September. Oxfam (2008) reported that farmers in Uganda observe an increasingly inconsistent rainfall pattern in the MAM season often resulting into drought and crop failure, but also more extreme rainfall during the OND season at the end of the year, causing flooding and erosion.

Local level studies conducted in Uganda to provide evidence of changing climate have focused mostly on trends in daily, monthly, seasonal and annual rainfall (Ogwang *et al.,* 2012; Mubiru *et al.,* 2012; Nsubuga *et al.,* 2014; Kansiime *et al.,* 2013; Kizza *et al.,* 2009; Stampone *et al.,* 2011; Diem *et al*., 2014; Osbahr *et al*., 2011). Majority of these reveal that rainfall has significantly declined in the cattle corridor axis (stretching from the Karamoja region in the Northeast, through Central, down to the Ankole region in the Southwest); conversely, an increase in rainfall is evident in Eastern Uganda (Mt. Elgon region) and parts of Lake Victoria basin.

Climatic trends are limited to describing patterns in only univariate data, yet a rainfall season is defined by observations from more than one variable (month). As such, climate trend analyses yield little information about changes in rainfall seasons over time. This study addressed the gap by using spatial analysis as well as multivariate analysis techniques on historical rainfall data to simultaneously examine changes across the major rainy seasons, as a way of providing evidence of rainfall change over Uganda.

This study has identified the potential hotspots of rainfall change over Uganda with focus on March-May (MAM) and October-December (OND) seasons. We have determined the geographic areas in Uganda whose seasonal rainfall over the past three decades (1981-2010) deviates from the long-term mean. Data quality control was undertaken on the acquired historical rainfall data for the identified areas. Finally, we carried out detailed statistical analysis on the historical datasets to determine evidence of rainfall change in the identified areas.

Methodology

Uganda lies in East Africa, astride the equator with its area lying between latitude $4^0$12'N and $1^0$29'S and longitude $29^0$34'W and $35^0$0'E. It has an estimated total area of 241,040 Km^2 and its altitude ranges between 620 m (Albertine Rift) and 5110 m (Mt. Rwenzori), with a mean of 1200 m above sea level. Uganda's climate is typically tropical with moderate variation in temperature throughout the year. Uganda has five climatic zones, which include: the Lake Victoria basin, the Karamoja region, Western Uganda, the Acholi-Kyoga region and the Ankole-southern area. Distinctive wet and dry seasons characterize most of the country's climate, except in the semi-arid northeast. Annual rainfall and temperature range from 700 mm to 3000 mm; and 16 ^{0}C to 31 ^{0}C, respectively and show variation depending on elevation and landscape (NEMA, 2010).

Monthly rainfall records for selected meteorological stations (Figure 1) across Uganda for the period extending from 1951 to 2010 were used in this study. The data were acquired from Uganda National Meteorological Authority (UNMA) database. The stations used were selected basing on data availability and representation of the homogenous rainfall zones defined by Basalirwa (1995).

Gaps in existing historical weather data alluding to stolen or old equipment and shortage of trained observers confounds climate change related analyses. This problem was addressed by filling the gaps using satellite-based observations and automated weather data in line with suggestions by Komutunga *et al.*, (2015). Modern-Era Retrospective Analysis for Research and Applications (MERRA) satellite data at 0.25 degree resolution were acquired from the National Aeronautics and Space Administration (NASA), while automated weather data were obtained from Adcon telemetry database of the National Agricultural Research Organization (NARO). The satellite/automated data were adjusted for differences in location and time of observation and then compared to manual (station) records using linear regression methods. Locations whose observations correlated strongest with actual data were then used to estimate the missing data.

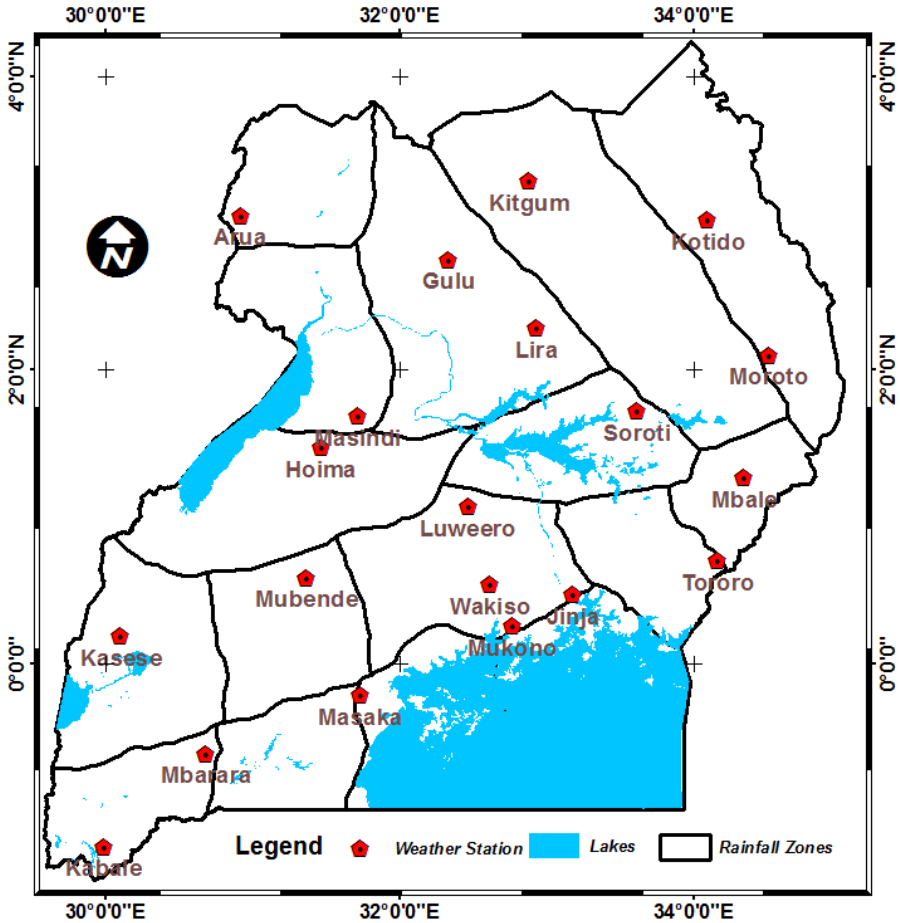

Figure 1: *Distribution of meteorological stations by homogenous rainfall zones (Basalirwa, 1995) from which the stations used in the study were selected*

Deviations from long-term (1951-2010) mean rainfall totals during the major rainy seasons for the decades 1981-1990, 1991-2000 and 2001-2010 were mapped using Geospatial climate data-management and analysis (GeoCLIM) tool designed for studying historical rainfall and temperature changes. It contains both national and regional gridded rainfall and temperature time-series that were developed by blending geostationary thermal infrared imagery (0.05 degree spatial resolution) with station observations using robust geo-statistical methods (Galu, 2014).

The main problem with time series from station data is that they are often not homogeneous as they exhibit trends or sudden jumps in the mean or variance. This may be caused by changes in the: observing site, observing equipment, observing procedures and time, and personnel. Any conclusions drawn from analyzing such data may thus be biased (von Storch and Zwiers, 2001). In this study, two methods were used to detect departures from homogeneity in the rainfall series for the identified areas: namely Standard Normal Homogeneity Test (SNHT) for a single break and Pettit test. These two tests are capable of locating the time (year) where a break is likely. The SNHT detects breaks near the beginning and the end of a series relatively easily, whereas the

Pettit test is more sensitive to breaks in the middle of a time series (Wijngaard *et al.*, 2003). The following hypotheses on homogeneity were tested:

H_0: The values x_i of the testing variable X are homogenous
H_A: A step-wise shift in the mean (a break) is present

Data Analysis

Standard Normal Homogeneity Test (SNHT)

Alexandersson (1986) describes a statistic *T(k)* for detecting a shift in the mean value of a time-series by comparing the mean of the first k years of the record with that of the last $n - k$ years:

$$T(k) = k\bar{Y}_1^2 + (n-k)\bar{Y}_2^2 \qquad k = 1, \ldots, n \tag{1}$$

where

$$\bar{Y}_1 = \frac{1}{k}\sum_{i=1}^{k}\left(X_i - \bar{X}\right)/s \quad \text{and} \quad \bar{Y}_2 = \frac{1}{n-k}\sum_{i=k+1}^{n}\left(X_i - \bar{X}\right)/s \tag{2}$$

where $\bar{X}$ and s are the estimated mean and standard deviation of observations x_i respectively.
If a break is located at the year K, then *T(k)* reaches a maximum near the year $k = K$. This is depicted in the graphs representing the results of this test. The test statistic T_0 is defined as:

$$T_0 = \max_{1 \le k < n} T(k) \tag{3}$$

The null hypothesis H_0 is rejected if T_0 is above a certain level, which is dependent on the sample size as shown by the critical values in Table 1.

Table 1: 1% and 5% critical values for the test statistic T_0 of the single shift SNHT

n	**20**	**30**	**40**	**50**	**60**	**70**	**100**
T_{95}	7.089	7.747	8.151	8.432	8.647	8.814	9.167
T_{99}	9.113	10.153	10.771	11.193	11.498	11.737	12.228

Source (Khaliq and Ouarda, 2007)

Pettitt Test

This approach by Pettitt (1979) is commonly applied to detect a single change-point in a time-series with continuous data. For T observations, the test statistic is defined as:

$$K_T = \max |U_{t,T}|, \quad 1 \le t \le T \tag{4}$$

$$\text{where} \quad U_{t,T} = \sum_{i=1}^{t}\sum_{j=t+1}^{T} \operatorname{sgn}\left(x_i - x_j\right) \quad \text{in which} \quad \operatorname{sgn}(x) = \begin{cases} 1 & \text{if } x > 0 \\ 0 & \text{if } x = 0 \\ -1 & \text{if } x < 0 \end{cases} \tag{5}$$

The change-point of the series is located at t, provided that the statistic is significant.

Evidence of rainfall change in the identified areas was determined by making simultaneous comparison of mean seasonal rainfall between two sub-periods of time. The sub-periods compared were each of length thirty years, in line with the recommended minimum baseline period for climatological assessments by the World Meteorological Organization (WMO, 1996).

A multivariate analysis approach was used where each rainfall season was assumed to constitute p x 1 and q x 1 random vectors representing the first and second sub-periods (groups) respectively. The variables measured on each unit (year of observation) were total rainfall in Mar, Apr and May or Oct, Nov and Dec. Since each rainfall season is made up of *three* months, it implies that $p = q = 3$, thus yielding a *three*-variate data structure as illustrated below:

Let $\mathbf{y}$ be an observation vector containing monthly total rainfall of a single rainfall season for the two sub-periods to be compared:

$$\mathbf{y} = \begin{pmatrix} \mathbf{y}_1' \\ \mathbf{y}_2' \end{pmatrix} = \begin{bmatrix} Y_{11} & Y_{12} & Y_{13} \\ Y_{21} & Y_{22} & Y_{23} \end{bmatrix} \tag{6}$$

where $\mathbf{y}_1$ and $\mathbf{y}_2$ are sub-vectors (each of dimension *3* x 1) representing the months of a particular rainfall season in the first and second sub-periods respectively.

Multivariate Two-sample Hotelling T^2 test

The rainfall mean vectors defining MAM and OND seasons were compared between two sub-periods of time using Multivariate Two-Sample Hotelling's T^2-test (Hotelling, 1951), a special case of the One-way Multivariate Analysis of Variance (MANOVA) model. The statistical differences between the mean vectors were tested as described below by Rencher (2003).

The Hotelling's T^2-test assumes that

(i) In each population, the variables have a multivariate normal distribution,
(ii) the observations are independent in each population, and
(iii) the populations have the same covariance matrix

Assumption (i) was checked using chi-square plots of standardized distances $\mathbf{D}_i^2$ from the mean vector (Mahalanobis distances) against Chi-square (χ^2) quantiles.

$$\mathbf{D}_i^2 = \left(\mathbf{y}_i - \bar{\mathbf{y}}\right)'\mathbf{S}^{-1}\left(\mathbf{y}_i - \bar{\mathbf{y}}\right) \qquad i = 1, 2, \ldots, n \tag{7}$$

where $\mathbf{y}_i$ is the data vector containing seasonal rainfall observations for a particular sub-period, $\bar{\mathbf{y}}$ is the sample mean vector and $\mathbf{S}$ is the sample covariance matrix. A non-linear pattern in the plot would indicate a departure from multivariate normality while points close to a straight line indicate no deviation from the assumption.

Assumption (ii) was tested by checking the independence of two sub-vectors. Suppose the observation vector $\mathbf{y}$ is partitioned into two sub-vectors of interest $\mathbf{y}_1$ and $\mathbf{y}_2$ of dimension $p \times 1$

and q x 1 respectively, as shown in equation (6). The corresponding partitioning of the population and sample covariance matrices is

$$\mathbf{\Sigma} = \text{cov}\begin{pmatrix}\mathbf{y}_1\\ \mathbf{y}_2\end{pmatrix} = \begin{pmatrix}\mathbf{\Sigma}_{11} & \mathbf{\Sigma}_{12}\\ \mathbf{\Sigma}_{21} & \mathbf{\Sigma}_{22}\end{pmatrix}, \qquad \mathbf{S} = \begin{pmatrix}\mathbf{S}_{11} & \mathbf{S}_{12}\\ \mathbf{S}_{21} & \mathbf{S}_{22}\end{pmatrix} \tag{8}$$

The hypothesis of independence of sub-vectors $\mathbf{y}_1$ and $\mathbf{y}_2$ can be expressed as

$$H_{01}: \mathbf{\Sigma}_{12} = \mathbf{O} \qquad \text{vs.} \qquad H_{11}: \mathbf{\Sigma}_{12} \neq \mathbf{O}$$

which means that every variable in $\mathbf{y}_1$ is independent of every variable in $\mathbf{y}_2$. The likelihood ratio test statistic for H_{01} is given by

$$\Lambda = \frac{|\mathbf{S}|}{|\mathbf{S}_{11}||\mathbf{S}_{22}|} \tag{9}$$

which is distributed as $\Lambda_{p,\,q,\,n-1-q}$. At $\alpha = 0.05$, $\boldsymbol{H}_{01}$ is rejected if $\Lambda \leq \Lambda_{0.05}$.
The critical values for Wilks' Λ at 5% significance level were obtained from Rencher (2003).

Assumption (iii) was tested as follows:

$$H_{02}:\ \mathbf{\Sigma}_1 = \mathbf{\Sigma}_2 \qquad \text{vs.} \qquad H_{12}:\ \mathbf{\Sigma}_1 \neq \mathbf{\Sigma}_2$$

where $\mathbf{\Sigma}_1 = \text{cov}(\mathbf{y}_1)$ and $\mathbf{\Sigma}_2 = \text{cov}(\mathbf{y}_2)$ (10)

Assuming independent samples of size n_1 and n_2 from multivariate normal populations, and defining the corresponding degrees of freedom as v_1 and v_2, the test statistic u is computed by chi-square approximation as follows:

$$u = -2(1-c)\ln M \tag{11}$$

where $c = \dfrac{(k+1)(2p^2+3p-1)}{6kv(p+1)}$ and $M = \dfrac{|\mathbf{S}_1|^{v_1/2}|\mathbf{S}_2|^{v_2/2}}{|\mathbf{S}_p|^{(v_1+v_2)/2}}$ (12)

in which $v_1 = n_1 - 1$ and $v_2 = n_2 - 1$, $\mathbf{S}_1$ and $\mathbf{S}_2$ are the covariance matrices of the first and second samples respectively, $\mathbf{S}_p$ is the pooled sample covariance matrix (equation 15) and $p = 3(\text{variables})$ $k = 2(\text{groups})$ and $v_1 = v_2 = v$

Choosing $\alpha = 0.05$, the computed statistic u is then compared with $\chi^2\left[0.05,\ 1/2(k-1)p(p+1)\right]$

The null hypothesis H_{02} is rejected if $u > \chi^2_{0.05}$ or if the p-value < 0.05.

Having affirmed that the data are independent, multivariate normal and that the covariance matrices are equal, the hypothesis for equality of mean vectors was then tested as shown below:

$$H_{03}: \boldsymbol{\mu}_1 = \boldsymbol{\mu}_2 \qquad \text{vs.} \qquad H_{13}: \boldsymbol{\mu}_1 \neq \boldsymbol{\mu}_2$$

where $\boldsymbol{\mu}_1 = \mathrm{E}(\mathbf{y}_1)$ and $\boldsymbol{\mu}_2 = \mathrm{E}(\mathbf{y}_2)$ (13)

Assuming the *first* sub-period of time forms a random sample $\mathbf{y}_{11}, \mathbf{y}_{12}, \ldots, \mathbf{y}_{1n_1}$ from $N_3(\boldsymbol{\mu}_1, \boldsymbol{\Sigma}_1)$ and the *second* sub-period also forms a random sample $\mathbf{y}_{21}, \mathbf{y}_{22}, \ldots, \mathbf{y}_{2n_2}$ from $N_3(\boldsymbol{\mu}_2, \boldsymbol{\Sigma}_2)$ the first step is to compute the sample mean vectors:

$$\bar{\mathbf{y}}_1 = \sum_{i=1}^{n_1} \mathbf{y}_{1i} / n_1 \quad \text{and} \quad \bar{\mathbf{y}}_2 = \sum_{i=1}^{n_2} \mathbf{y}_{2i} / n_2 \tag{14}$$

Since $(n_1 - 1)\mathbf{S}_1$ and $(n_2 - 1)\mathbf{S}_2$ are unbiased estimators of $(n_1 - 1)\boldsymbol{\Sigma}$ and $(n_2 - 1)\boldsymbol{\Sigma}$ respectively, they can be pooled to obtain an unbiased estimator $\mathbf{S}_p$ of the common population covariance matrix $\boldsymbol{\Sigma}$:

$$\mathbf{S}_p = \frac{(n_1 - 1)\mathbf{S}_1 + (n_2 - 1)\mathbf{S}_2}{n_1 + n_2 - 2} \tag{15}$$

The multivariate two-sample Hotelling's T^2-statistic is obtained as:

$$T^2 = \frac{n_1 n_2}{n_1 + n_2} \left(\bar{\mathbf{y}}_1 - \bar{\mathbf{y}}_2\right)' \mathbf{S}_p^{-1} \left(\bar{\mathbf{y}}_1 - \bar{\mathbf{y}}_2\right) \tag{16}$$

which is distributed as $T^2_{p, n_1 + n_2 - 2}$ when $\boldsymbol{H_{03}}$ is true.

The Multivariate Two-Sample Hotelling's T^2-test is a special case of the One-way MANOVA model, where population mean vectors of two groups (k = 2) are compared. Following this relationship, the Hotelling T^2-statistic can be transformed to an approximate F-statistic as follows

$$F = \frac{n_1 + n_2 - p - 1}{(n_1 + n_2 - 2)p} T^2 \sim F_{p,\ n_1 + n_2 - p - 1} \tag{17}$$

At 5% significance level, H_{03} is rejected if $F > F_{[0.05,\ p,\ n_1 + n_2 - p - 1]}$ or if $p < 0.05$.

Suppose that the Hotelling T^2-test leads to the rejection of $\boldsymbol{H_{03}}$, the discriminant function coefficient vector $\mathbf{a}$ is computed in order to determine the individual *variables* (months) that contribute most to separation of the two groups (sub-periods)

$$\mathbf{a} = \mathbf{S}_p^{-1} \left(\bar{\mathbf{y}}_1 - \bar{\mathbf{y}}_2\right) \tag{18}$$

Findings

Identification of potential hotspot areas of rainfall change over Uganda

Seasonal rainfall totals during the decades 1981-1990, 1991-2000 and 2001-2010 were spatially compared to the long-term mean (1951-2010) to detect any departures.

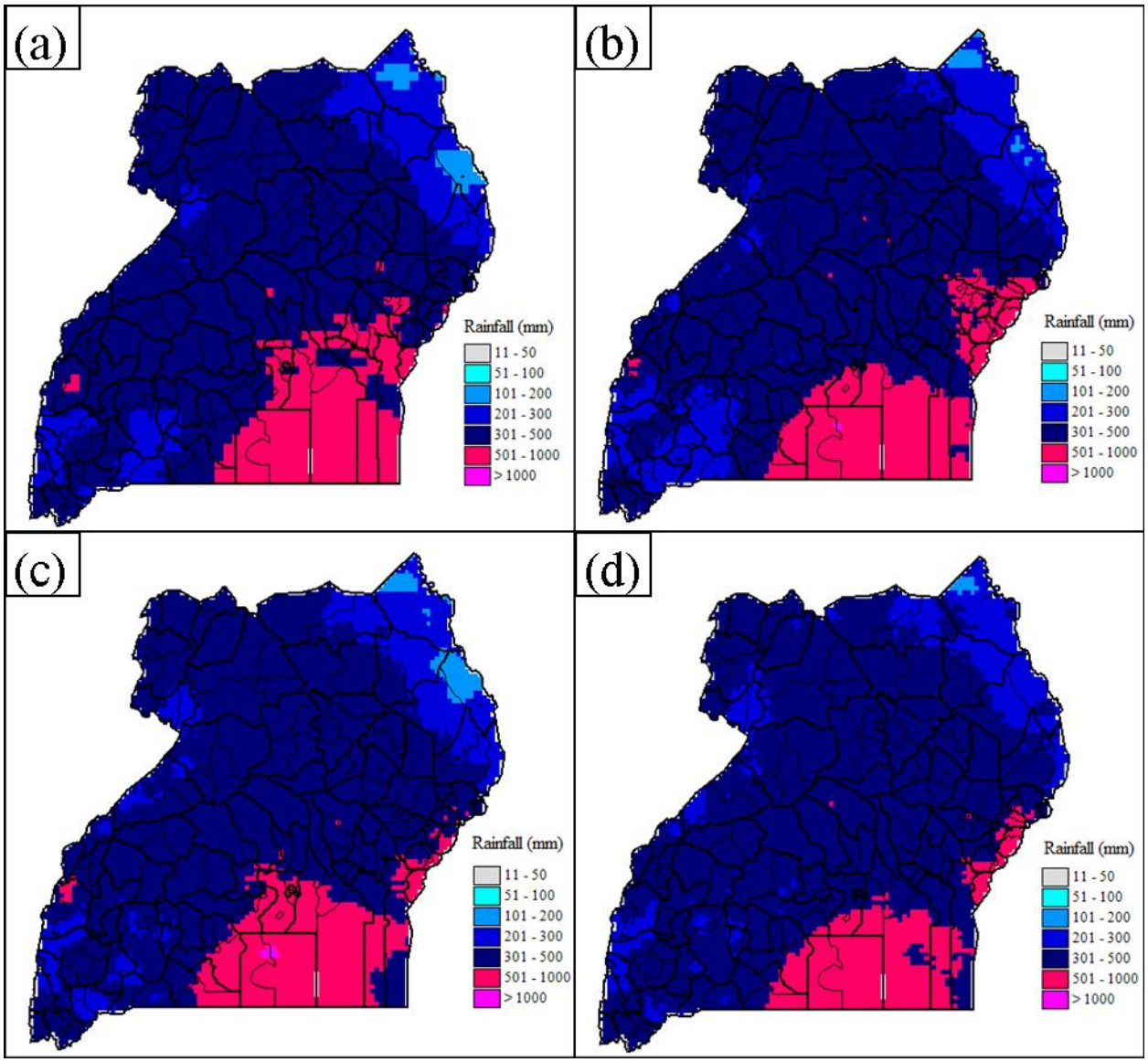

Figure 2: *Average total rainfall over Uganda during the MAM season for (a) long-term period, (b) 1981-1990, (c) 1991-2000, and (d) 2001-2010*

Compared to the long-term period, rainfall during the MAM season was observed to have increased in areas around L. Victoria basin and Mt Elgon region in Eastern Uganda in each of the last three decades (Figure 2). This is shown by the expansion in areas receiving over 500 mm of rainfall during this season. However, Karamoja sub-region in Northeastern Uganda continues to experience low rainfall (below 200 mm) while some parts in the Southwest have shown a decline in volume of MAM rainfall from 301 mm - 500 mm down to 201 mm - 300 mm.

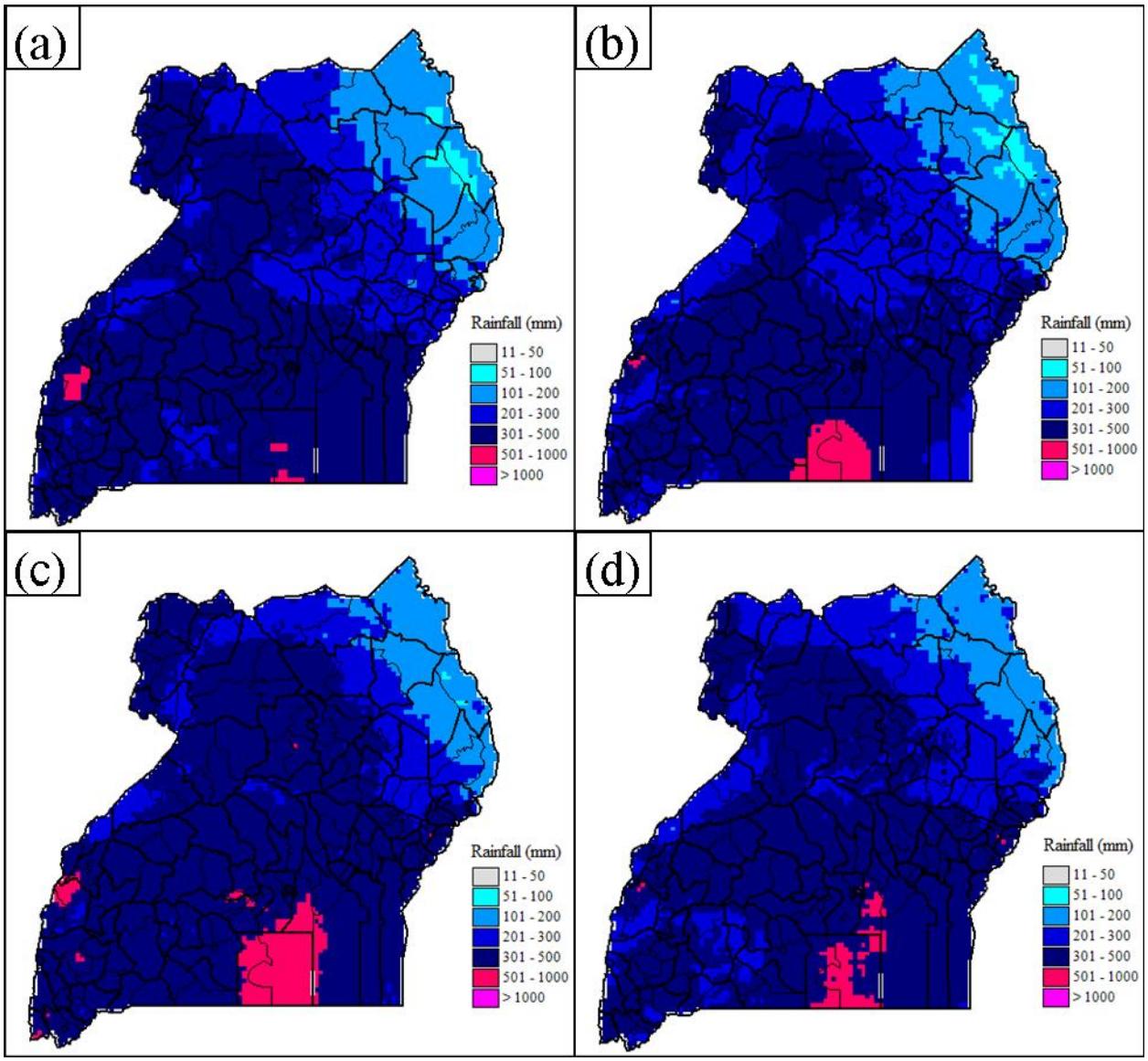

Figure 3: *Average total rainfall over Uganda during the OND season for (a) long-term period, (b) 1981-1990, (c) 1991-2000 and (d) 2001-2010*

Contrary to the MAM season, rainfall during the OND season showed no drastic changes from its long-term mean (Figure 3). However, rainfall increases during this season were spotted for most parts of the country as shown by the expansion in areas receiving over 300 mm particularly in Eastern Uganda, while low rainfall continues to dominate the country's Northeastern parts.

Selected areas for further analysis of hotspots of rainfall change

Following the spatial analysis results of changes in seasonal rainfall over Uganda as presented by Figures 2 and 3, areas that showed notable departure from long-term mean rainfall were selected for further investigation in order to provide evidence of change. Table 2 gives a brief description of meteorological stations that were used for this task.

Table 2: Selected meteorological stations for further analysis of rainfall change hotspots

Station name	District	Latitude (decimal ^{0})	Longitude (decimal ^{0})	Elevation (m)	Region
Mbale forest station	Mbale	1.267	34.350	1875	Eastern (Mt. Elgon)
Nabilatuk Station	Moroto	2.100	34.517	1250	Northeastern (Karamoja)
Mbarara Met Station	Mbarara	-0.617	30.683	1420	Southwestern

Quality control on historical rainfall data for the identified areas

Historical rainfall datasets for the stations representing the identified hotspot areas were tested for inhomogeneities and found to be homogeneous by both SNHT and Pettit tests (Table 3). The computed values from the SNHT statistic were all less than the critical value (8.647) while the *p*-values from Pettitt test were greater than 0.05, thus providing no sufficient evidence against the assumption of homogeneity. The data were therefore fit to be used for further statistical analyses.

Table 3: Homogeneity test results for historical monthly rainfall data

District (Region)	Rainfall Season		SNHT (n=60) Score (T_0)*	Pettitt Test (n=60) K	p-value
Mbale (Mt. Elgon)	Long-rains	Mar	7.174	236	0.437
		Apr	5.824	187	0.769
		May	6.364	238	0.426
	Short-rains	Oct	3.333	244	0.393
		Nov	6.560	208	0.613
		Dec	5.915	236	0.437
Moroto (Karamoja)	Long-rains	Mar	2.673	172	0.891
		Apr	5.316	194	0.715
		May	2.966	198	0.685
	Short-rains	Oct	2.727	265	0.294
		Nov	5.368	195	0.708
		Dec	4.387	241	0.409
Mbarara (Southwestern)	Long-rains	Mar	5.341	213	0.579
		Apr	5.023	285	0.217
		May	4.604	226	0.495
	Short-rains	Oct	4.452	201	0.663
		Nov	6.737	255	0.338
		Dec	6.971	293	0.193

**Test carried out at 95% confidence level, critical value T_{95} = 8.647*

Determining evidence of rainfall change in the identified areas

In order to provide evidence of rainfall change in the selected (hotspot) areas, the mean vectors defining seasonal rainfall were compared between the sub-periods 1951-1980 and 1981-2010 using MANOVA and Hotelling T^2-test whose assumptions were first checked as described below

- **Checking for multivariate normality**

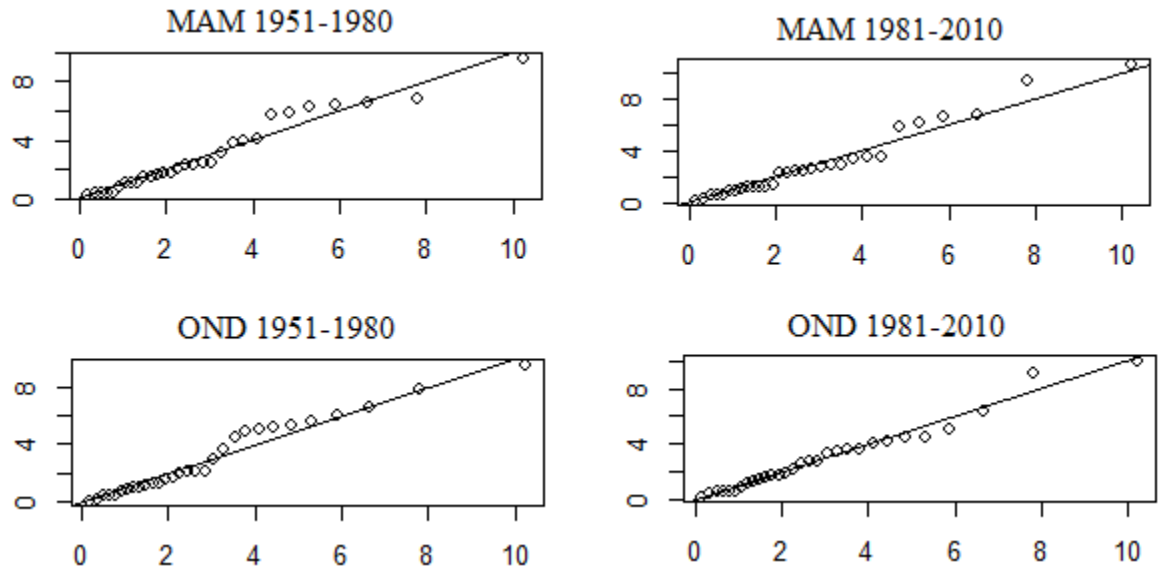

Figure 4(a)*: Plot of Mahalanobis distances against chi-square quantiles for* ***Mbale*** *rainfall*

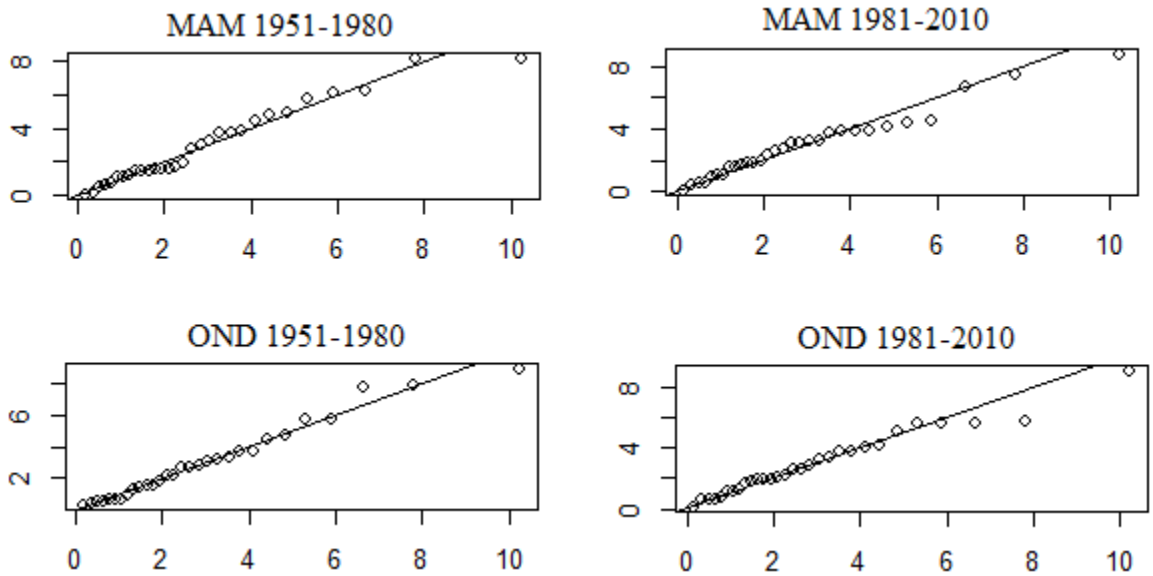

Figure 4(b)*: Plot of Mahalanobis distances against chi-square quantiles for* ***Mbarara*** *rainfall*

The chi-square plots for MAM and OND seasons over Mbale and Mbarara areas showed no notable deviations from linearity (Figures 4(a) and 4(b)). This implied that the total rainfall for the months defining each season followed a multivariate normal distribution in each sub-period.

For cases where the assumption of multivariate normality was violated such as OND rainfall in Moroto, Hotelling T^2 and MANOVA were still applied since these tests have been found to be fairly robust to departures from multivariate normality and heterogeneity of covariance matrices as long as the sample sizes are large and equal (Rencher, 2003).

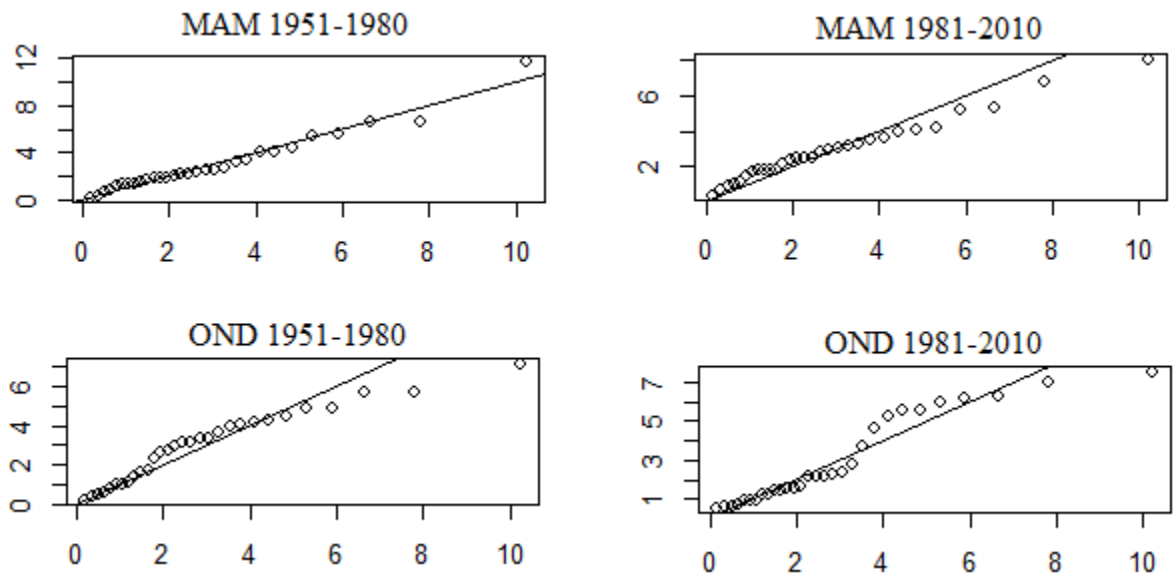

Figure 4(c)*: Plot of Mahalanobis distances against chi-square quantiles for* ***Moroto*** *rainfall*

➢ **Testing for independence and equality of covariance matrices between sub-periods**

There was no sufficient evidence against the assumption of independence in monthly rainfall observations between the sub-periods 1951-1980 and 1981-2010 ($\Lambda > 0.514$). In addition, the rainfall covariance matrix for 1951-1980 did not significantly differ ($p > 0.05$) from that of 1981-2010 implying that pooling of the covariance matrices was statistically viable (Table 4).

Table 4: Test results for independence and equality of covariance matrices between sub-periods

Attribute	**Hotspot area**	**Season** (n = 30)	**Testing $\Sigma_{12} = O$**	**Testing $\Sigma_1 = \Sigma_2$**	
			Wilk's Λ*	u	p-value**
Rainfall	Mbale	MAM	0.750	4.205	0.649
		OND	0.720	3.187	0.785
	Mbarara	MAM	0.609	10.618	0.101
		OND	0.515	3.686	0.719
	Moroto	MAM	0.724	3.280	0.773
		OND	0.692	6.227	0.398

**Critical value $\Lambda_{[0.05,3,3,26]} = 0.514$; **Computed by chi-square approximation*

Testing for difference in mean vectors

The rainfall mean vector for 1951-1980 significantly differed ($p < 0.05$) from that of 1981-2010 in all the areas during the MAM season (Table 5). In particular, mean rainfall in Mbale was observed to have simultaneously increased the MAM season, with April having the highest increase (*largest absolute coefficient*) of about 10 mm. On the contrary, mean rainfall in Mbarara and Moroto was found to have decreased jointly across the MAM season, with April experiencing the greatest decrease (18 mm and 11 mm respectively).

Table 5: Two-sample Hotelling T^2-test results for rainfall change in the selected hotspot areas

Hotspot	Season	Rainfall (mm)		Testing $\mu_1 = \mu_2$ (n = 30)			Discriminant
		1951-1980	1981-2010	T^2	F*	p-value	*Coefficient*
Mbale	Mar	76.47	79.16	129.698	41.742	<0.001	–0.044
	Apr	159.46	169.45				–0.358
	May	183.60	200.23				–0.297
	Oct	146.08	156.26	42.658	13.729	<0.001	–0.250
	Nov	111.44	115.13				–0.061
	Dec	40.29	46.19				–0.112
Mbarara	Mar	100.17	95.77	65.003	20.92	<0.001	0.142
	Apr	128.95	110.78				0.177
	May	68.34	60.49				0.063
	Oct	119.61	114.42	8.333	2.682	0.056	
	Nov	158.98	155.66				N/A
	Dec	66.24	66.63				
Mororo	Mar	51.83	43.04	28.416	9.145	<0.001	0.083
	Apr	92.69	81.78				0.101
	May	124.31	121.17				0.022
	Oct	66.16	66.31	7.327	2.358	0.081	
	Nov	55.12	54.38				N/A
	Dec	20.00	26.72				

**Approximated value of statistic* *N/A = Not Applicable*

For the OND season, the rainfall mean vector for 1951-1980 was not significantly different ($p > 0.05$) from that of 1981-2010 in Mbarara and Moroto areas. Only mean rainfall in Mbale was observed to have significantly increased ($p < 0.05$) across all months of the OND season, with October experiencing the highest increase (*largest absolute coefficient*) of about 10 mm.

Discussion

This study found that the historical monthly rainfall series for the identified hotspot areas in Uganda over the period 1951-2010 were homogenous and therefore useful for further analysis. The homogenous and good quality climate data has also been observed in previous studies by Mubiru *et al.*, (2012), Kizza *et al.*, (2009), Basalirwa (1995) and Nsubuga *et al.*, (2014) who used various methods such as residual mass curves, Buishand test and von Neumann ratio.

The present study found that rainfall during the MAM season has generally declined in Northeastern and Southwestern Uganda over the last three decades relative to the long-term mean. This was confirmed by the significant simultaneous decrease in mean rainfall across all months of this season particularly during April for Moroto and Mbarara areas over the period 1981-2010. Similar results were obtained by Mubiru *et al.*, (2012) who noted a decline in rainfall volume for the months of April and May over the period 1950-2008 in bimodal-regime dominated areas. The results are also consistent with findings by Stampone *et al.*, (2011) and Diem *et al*., (2014), who observed significant decrease in rainfall amount received in Western Uganda during the long-rains season over the periods 1941-1975 and 1983-2012 respectively. The results however differ from findings by Osbahr *et al.*, (2011) and Nsubuga *et al.*, (2014) who reported insignificant changes in monthly rainfall over Mbarara district (1963-2008) and Southwestern region (1943-1977) respectively during MAM season.

Unlike the MAM season, the current study revealed that rainfall during the OND season did not exhibit a similar (decreasing) pattern over Moroto and Mbarara areas as illustrated by the insignificant difference in OND rainfall mean vectors between 1951-1980 and 1981-2010. These results do not concur with findings by Mubiru *et al.*, (2012), who reported a significant decline in rainfall amount received in Karamoja region during the OND season over the period 1950-2008. This disparity in findings could be attributed to the difference in time periods used and the fact that this study used monthly rainfall while Mubiru *et al.*, (2012) used daily rainfall records.

Contrary to Northeastern and Southwestern Uganda where rainfall has declined, this study indicated that areas around Mt Elgon and Eastern Uganda in general, have experienced notable increments in MAM and OND rainfall over the past three decades. This was affirmed by the simultaneous significant increase in mean rainfall across all months defining both wet seasons for Mbale area over the period 1981-2010 particularly during April and October. The results compare well with findings by Kansiime *et al.*, (2013) and Kizza *et al.*, (2009) who observed a significant rise in volume of rainfall received during both wet seasons over Mt Elgon region (1971-2010) and Northeastern parts of L. Victoria basin (1941-2008) respectively. The results are also in line with suggestions by Ogwang *et al.*, (2012) who noted that L. Victoria and L. Kyoga basins as well as Eastern parts of Uganda were dominated by high flood incidences over the period 1962-2007 especially during the short-rains season.

Conclusion and Recommendation

From the results, the study concludes that hotspots of rainfall decrease were evident only during the MAM season in areas of Moroto in Karamoja (Northeastern Uganda) and Mbarara in Southwestern region. On the other hand, hotpots of rainfall increase occurred during both MAM and OND seasons and were prominent in Mbale in Mt Elgon region (Eastern Uganda).

The information generated from this study could be used as a decision making tool by research scientists and policy makers in prioritizing areas in Uganda where adaptation action is needed most in an effort to combat impacts of climate change.

Unlike the rest of the country with a bimodal rainfall pattern, areas far north of Uganda experience a unimodal rainfall pattern (April to September) as has been observed by Phillips and McIntyre (2000). There is need to account for this disparity by distinguishing between hotspots of unimodal and bimodal rainfall regimes.

References

Alexandersson, H. (1986). A homogeneity test applied to precipitation data. *Journal of climatology*, *6*(6), 661-675.

Basalirwa, C. P. K. (1995). Delineation of Uganda into climatological rainfall zones using the method of principal component analysis. *International Journal of climatology*, *15*(10), 1161-1177.

Diem, J. E., Ryan, S. J., Hartter, J., and Palace, M. W. (2014). Satellite-based rainfall data reveal a recent drying trend in central equatorial Africa. *Climatic Change*, *126*(1-2), 263-272.

Galu, G. (2014, December). Building Capacity for Production of Gridded Precipitation Products in the East Africa Community. In *2014 AGU Fall Meeting*. Agu.

GOU (2010). *National Development Report 2010/2011-2014/2015*. Government of Uganda (GOU), Kampala.

Hagenlocher, M., Lang, S., Holbling, D., Tiede, D., and Kienberger, S. (2014). Modeling hotspots of climate change in the Sahel using object-based regionalization of multidimensional gridded datasets. *Selected Topics in Applied Earth Observations and Remote Sensing, IEEE Journal of*, *7*(1), 229-234.

Hotelling, H. (1951), "A Generalized *T* Test and Measure of Multivariate Dispersion," *Proceedings of the Second Berkeley Symposium on Mathematical Statistics and Probability*, **1**, 23–41.

IPCC (2007), *Climate Change 2007: The Physical Science Basis*: Contribution of Working Group I to the Fourth Assessment Report of the Intergovernmental Panel on Climate Change (IPCC), edited by S. Solomon et al., Cambridge Univ. Press, Cambridge, U. K.

Kansiime, M. K., Wambugu, S. K., and Shisanya, C. A. (2013). Perceived and actual rainfall trends and variability in Eastern Uganda: Implications for community preparedness and response. *Journal of Natural Sciences Research*, *3*(8), 179-194.

Khaliq, M. N., and Ouarda, T. B. M. J. (2007). On the critical values of the standard normal homogeneity test (SNHT). *International Journal of Climatology*, *27*(5), 681-687.

Kizza, M., Rodhe, A., Xu, C. Y., Ntale, H. K., and Halldin, S. (2009). Temporal rainfall variability in the Lake Victoria Basin in East Africa during the twentieth century. *Theoretical and applied climatology*, *98*(1-2), 119-135.

Komutunga, E., Oratungye, J. K., Ahumuza, E., Akodi, D. and Agaba, C. (2015). New procedure in developing adjustment algorithm for harmonizing historical climate data sets. *Journal of Dynamics in Agricultural Research* 2(3):21-30,

Mubiru, D. N., Komutunga, E., Agona, A., Apok, A., and Ngara, T. (2012). Characterising agrometeorological climate risks and uncertainties: Crop production in Uganda. *South African Journal of Science*, *108*(3-4), 108-118.

Mukiibi, J.K., (Ed.) (2001). *Agriculture in Uganda*. General Information. Vol. 1, National Agricultural Research Organisation. Fountain Publishers Ltd., Kampala.

NEMA (2010). *State of the Environment Report for Uganda 2010*. National Environment Management Authority (NEMA), Kampala.

Nsubuga, F. N. W., Olwoch, J. M., and Botai, O. J. (2014). Analysis of mid-twentieth century rainfall trends and variability over southwestern Uganda. *Theoretical and applied climatology*, *115*(1-2), 53-71.

Ogwang, B. A., Guirong, T., and Haishan, C. (2012). Diagnosis of September–November drought and the associated circulation anomalies over Uganda. *Pakistan Journal of Meteorology*, *9*(2).

Osbahr, H., Dorward, P., Stern, R., and Cooper, S. (2011). Supporting agricultural innovation in Uganda to respond to climate risk: linking climate change and variability with farmer perceptions. *Experimental Agriculture*, *47*(02), 293-316.

Pettitt, A. N. (1979). A non-parametric approach to the change-point problem. *Applied statistics*, 126-135.

Phillips, J., and McIntyre, B. (2000). ENSO and interannual rainfall variability in Uganda: implications for agricultural management. *International Journal of Climatology*, *20*(2), 171-182.

Rencher, A. C. (2003). *Methods of multivariate analysis* (Vol. 492). John Wiley & Sons.

Stampone, M. D., Hartter, J., Chapman, C. A., and Ryan, S. J. (2011). Trends and variability in localized precipitation around Kibale National Park, Uganda, Africa. *Research Journal of Environmental and Earth Sciences*.

Thornton, P. K., Jones, P. G., Owiyo, T., Kruska, R. L., Herrero, M., Orindi, V., ... and Omolo, A. (2008). Climate change and poverty in Africa: Mapping hotspots of vulnerability. *African Journal of Agricultural and Resource Economics*, *2*(1), 24-44.

von Storch, H. and Zwiers, F. W. (2001). *Statistical analysis in climate research*. Cambridge university press.

Wijngaard, J. B., Klein Tank, A. M. G., and Können, G. P. (2003). Homogeneity of 20th century European daily temperature and precipitation series. *International Journal of Climatology*, *23*(6), 679-692.

WMO (1996). *Climatological Normals (CLINO) for the period 1961–1990*. World Meteorological Organization: Geneva, Switzerland.